# ESP32-based Car Battery Drainage Detection and Selective Load Control System with GSM Alert Mechanism

Aayush Khatu, Tanay Bhamare, Manasi Nanaware, Anya Teli, Anup Date
Department of Electronics and Communication Engineering,
MIT ADT University, Pune, India

## ABSTRACT

Battery depletion in stationary vehicles is one of the most common reasons for automotive breakdowns worldwide. When a vehicle stays parked for long periods, the cumulative current drawn by control units, telematics modules, alarm systems, and other always-active electronics can quietly drain the 12 V lead-acid starter battery to the point where the engine cannot start. Current solutions—such as dashboard voltage gauges, Bluetooth-connected monitors, and proprietary OEM telematics—are mainly passive; they observe and report but do not actively stop the discharge process. This paper presents and experimentally validates a fully integrated, microcontroller-driven battery protection system based on the ESP32 system-on-chip and the SIM800L quad-band GSM module. The system continuously monitors battery terminal voltage using a precision resistive voltage-divider circuit and applies a dual-threshold detection algorithm. An SMS alert is sent via the cellular network when the voltage drops below 11.8 V; when the voltage reaches 11.2 V, a staged relay-based load-disconnection sequence is triggered. The ESP32 operates mainly in deep sleep mode, consuming only 48 µA when idle. Prototype tests on a 45 Ah flooded lead-acid battery showed an RMSE of 0.038 V, average SMS delivery time of 4.3 seconds, and successful staged relay load disconnection. Following load shedding, functional battery life was extended 4.7×. Total component cost is approximately ₹1,850 (US$22), making this solution affordable for retrofitting in conventional vehicles.

## General Terms

Embedded Systems, Automotive Electronics, Battery Management Systems, Internet of Things (IoT), GSM Communication, Energy Monitoring, Microcontroller-Based Systems.

## Keywords

ESP32; Vehicle Battery Protection; Smart Battery Management System; GSM Communication; SIM800L; Selective Load Isolation; Deep Sleep Mode; Lead-Acid Battery; Parasitic Drain; IoT-Embedded Systems; Relay Control; Threshold Detection

## 1. INTRODUCTION

The rise of embedded electronics in modern vehicles has created a persistent challenge: increased quiescent current draw from the 12 V lead-acid starter battery during parking. A typical mid-range vehicle may contain more than 70 Electronic Control Units (ECUs), each drawing power in standby mode even when the ignition is off. Industry standards permit a combined quiescent draw of 50–85 mA once all systems enter sleep mode; however, faults, aftermarket accessories, or aging can significantly raise this figure. Even compliant vehicles can drain a moderately sized lead-acid battery within two to four days of inactivity.

Roadside assistance data consistently shows that battery-related failures account for approximately 20–25% of all vehicle breakdowns. In India, where summer temperatures exceed 40 °C and many vehicles park outdoors without shade, thermal self-discharge compounds parasitic losses. The situation is further aggravated by the growing prevalence of aftermarket security systems, GPS trackers, and infotainment upgrades, all of which contribute additional quiescent current without the owner's awareness.

Existing protective solutions remain largely passive: dashboard voltage displays require manual inspection; Bluetooth battery monitors lose functionality when the paired smartphone is out of range; proprietary OEM battery management systems cannot be retrofitted; and cloud-connected telematics require constant data connectivity. Critically, none of these approaches offer autonomous load-shedding—they monitor but do not protect.

This paper addresses that gap with a purpose-built, closed-loop battery protection system combining: (a) a dual-threshold voltage-sensing algorithm that independently triggers early warnings and load disconnection; (b) a staged, relay-based selective load-isolation sequence that removes non-essential circuits by priority while preserving critical safety systems; and (c) an ultra-low-power operation strategy exploiting ESP32 deep sleep mode to reduce self-monitoring current to 48 µA. Remote notifications are delivered via the SIM800L GSM cellular module, providing nationwide coverage independent of Wi-Fi or smartphone proximity.

## 2. LITERATURE REVIEW

### A. IoT-Enabled Battery Monitoring Systems

The integration of microcontrollers with cloud connectivity for battery health monitoring has attracted substantial research interest during 2024–2025. Haldar et al. [1] developed an IoT-based BMS for electric vehicles using ESP32 with Arduino IoT Cloud, confirming the platform's suitability for BMS applications; however, their system targets lithium-ion EV batteries and requires continuous Wi-Fi connectivity, limiting applicability in offline parking scenarios. Kamble et al. [2] demonstrated ESP32-based battery monitoring via the Blynk mobile application, but similarly depends on persistent network access with no autonomous load-shedding capability. Islam et al. [3] presented a real-time monitoring solution specifically for conventional 12 V automotive batteries using IoT technologies—the most directly comparable work to this paper—though their design relies on Wi-Fi rather than cellular communication. Kontogiannis et al. [4] validated ESP32 DevKit v4 measurement accuracy and alert response times for lithium-ion battery modules, establishing performance benchmarks consistent with the targets of this system. Karthikeyen et al. [5] similarly reported an IoT-based wireless battery surveillance and management system, reinforcing the broader research interest in connected, always-on battery-monitoring architectures of the kind extended here with autonomous protection.

### B. Advanced BMS Architecture and State-of-Charge Estimation

Martinez et al. [6] presented a comprehensive IoT-integrated BMS using STM32/ESP32 for real-time SoC and SoH monitoring, published in the Elsevier Internet of Things journal (January 2025). Their hybrid MQTT/WebSocket communication architecture and cost-efficient design philosophy closely mirror the objectives of this work. Malele et al. [7] conducted a systematic review of 147 microcontroller-based BMS publications in IEEE Access (February 2025), establishing microcontroller-based control with wireless communication as the dominant emerging paradigm for BMS design. Bokstaller et al. [8] provided a comprehensive survey of IoT-based SoC, SoH, and remaining-useful-life estimation methods in the IEEE Internet of Things Journal (February 2025), contextualising the voltage-threshold approach adopted here. Ali et al. [9] developed and validated an adaptive CC/CV lithium-ion battery charger with real-time current monitoring in MDPI Technologies (May 2025), whose calibration methodology informed the prototype design. Mao et al. [10] proposed an equal-voltage-range sampling-count indicator for lithium-ion state-of-health estimation, illustrating the continued refinement of voltage-based diagnostic techniques that underpin the simpler threshold logic adopted in this work. Haraz et al. [11] surveyed machine-learning approaches to SoC and SoH estimation, noting the computational and data overhead such methods impose relative to lightweight, rule-based techniques suited to low-power embedded deployment. A related Scientific Reports study [12] combined IoT sensing, blockchain, and machine learning for EV battery management, illustrating the trend toward increasingly complex BMS architectures against which the low-cost, single-board design proposed here is positioned.

## C. GSM and Cellular Alert Systems in Embedded Applications

GSM-based notification systems continue to demonstrate high reliability in embedded protection applications. Pushpa et al. [13] developed a smart vehicle theft detection system using Arduino, NEO-6M GPS, and SIM800L GSM module, confirming reliable multi-network SMS delivery for vehicle security alerts—directly supporting the SIM800L selection in this paper. Khan and Alam [14] documented real-time asset and vehicle tracking using Arduino with GPS and GSM modules, confirming reliable alert delivery across field conditions regardless of service provider. Premkumar et al. [15] demonstrated the ESP32–SIM800L combination in an IoT video surveillance system, providing further evidence of this hardware pairing's communication reliability. Bokstaller et al. [8] concluded in their 2025 review that cellular communications offer the broadest geographic coverage for vehicle-monitoring data, reinforcing the GSM design choice over Wi-Fi.

## D. Power Optimisation and Deep Sleep Mode

The self-power consumption of a battery-monitoring system is a critical design variable—a monitor that exacerbates battery drain defeats its own purpose. Bhavya and Sudharshan [16] conducted a systematic analysis of ESP32-WROOM power consumption across communication interfaces and clock frequencies in ETASR (2025), reporting average current consumption below 50 µA using deep sleep with RTC timer wakeup—a result that directly validates the 48 µA idle current measured on the prototype in this work. Salim et al. [17] examined ESP32 power consumption in MQTT-based IoT systems across deep sleep and active modes (IEEE ICCE, 2025), confirming that deep sleep yields substantial power reduction despite increased wakeup latency. Karandikar et al. [18] demonstrated energy-efficient IoT hazard detection using ESP32-CAM with a 10-minute deep sleep wakeup interval in MDPI Sensors (March 2025), adopting duty-cycle optimisation strategies directly analogous to those used in this submission. Fikru et al. [19] provided the theoretical foundation for deep sleep adoption in MDPI Sensors (2024), confirming sleep-mode duty cycling as the most effective method for extending battery life in IoT nodes.

## E. IoT Monitoring and Control System Architectures

At a broader level, Majhi et al. [20] surveyed IoT applications across power systems generally, situating single-node battery-protection devices such as the one proposed here within the wider IoT power-monitoring ecosystem. Balcerak et al. [21] surveyed IoT-based monitoring and control systems across multiple domains in MDPI Applied Sciences (October 2024), identifying relay-based load control, threshold-triggered alerting, and SMS/cloud notification as the three foundational building blocks of embedded protection systems—precisely the architecture proposed in this paper. Raza et al. [22] reviewed sensing-based monitoring solutions for electric-vehicle batteries in Sensors and Actuators A: Physical (Elsevier, May 2025), highlighting voltage sensing, current sensing, and temperature sensing as foundational BMS elements, and explicitly identifying the absence of 12 V lead-acid battery research as a gap in the literature—a gap this paper directly addresses. Hassan et al. [23] described multi-relay, threshold-triggered protective system logic at IEEE IC2PCT 2024, whose staging strategy informed the relay-sequencing design adopted here.

## F. Research Gap and Novelty Statement

The literature survey reveals three persistent gaps in BMS research for 2024–2025: (1) the vast majority of BMS studies address lithium-ion EV batteries, with negligible coverage of lead-acid batteries in parked conventional vehicles that represent the global fleet majority; (2) existing monitoring systems alert but do not autonomously shed loads based on voltage state; and (3) the self-power consumption of monitoring hardware is rarely reported or minimised despite its direct relevance to battery preservation. The proposed prototype addresses all three gaps with a low-cost, autonomous, power-optimised design.

# 3. PROPOSED SYSTEM ARCHITECTURE AND HARDWARE DESIGN

## A. System Overview and Design Philosophy

The system is designed as an autonomous, standalone safety solution for any 12 V vehicle, requiring no modification to the vehicle's wiring harness (Figure 1). Five major components comprise the system: (1) a precision resistor voltage-sensing and signal-conditioning circuit; (2) an ESP32-WROOM-32 as CPU and decision engine; (3) a SIM800L GSM module for SMS notification; (4) a dual relay load-switching module for staged non-essential load disconnection; and (5) a 3.3 V regulated power supply derived from the monitored battery bus via a cascaded buck converter and LDO regulator. The fundamental design constraint is that the system must never worsen the battery-drain condition it is designed to prevent.

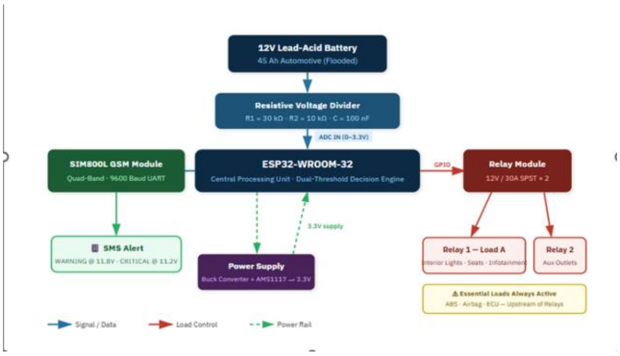


**Figure 1. Overall architecture of the proposed battery monitoring and selective load cutoff system**

## B. Voltage Sensing and Signal Conditioning

The ESP32 ADC pins accept a maximum of 3.3 V. A resistive voltage divider with R1 = 30 kΩ and R2 = 10 kΩ divides the battery voltage by four, mapping the 10.0 V–14.7 V automotive range to a 2.5 V–3.675 V ADC input range (Figure 2). A 100 nF capacitor in parallel with R2 attenuates high-frequency noise from the ignition system and alternator rectifier. Component values were selected to dissipate approximately 3.6 mW at 12 V—negligible over any practical monitoring interval.

Calibration used 50 reference readings between 10.0 V and 14.7 V with a NIST-traceable Fluke 87 V multimeter, yielding a second-order polynomial fit that corrects for known ESP32 ADC non-linearity near the upper input range [16]. Post-calibration accuracy was an RMSE of 0.038 V. Final voltage estimates are the average of 16 samples at 12-bit resolution, reducing quantisation noise below 2 mV effective—sufficient for accurate threshold discrimination at 11.2 V and 11.8 V.

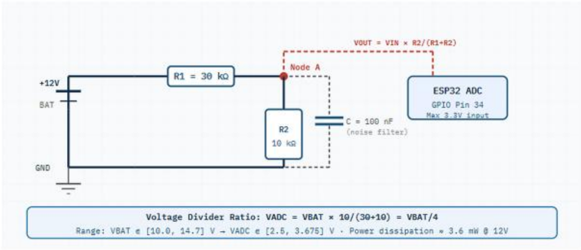


**Figure 2. Voltage sensing and signal conditioning circuit for ESP32 ADC interfacing**

## C. ESP32-WROOM-32 Microcontroller

The ESP32 was selected for its ultra-low deep sleep current (10–150 µA depending on RTC RAM retention), dual-core Xtensa LX6 processor, integrated 12-bit SAR ADC, and mature Arduino framework ecosystem [18][19]. Deep sleep with an RTC timer wakeup yields a typical idle current of 48 µA. The standard monitoring interval is 10 minutes; on threshold breach, the interval shortens to 60 seconds for faster recovery tracking. All GPIO peripherals are power-gated through a P-channel MOSFET controlled by an RTC GPIO, ensuring zero peripheral draw during sleep. Detailed electrical characteristics, timing diagrams, and peripheral specifications are documented in the manufacturer's technical reference manual [24].

## D. GSM Communication Module (SIM800L)

The SIM800L (SIMCom Wireless Solutions) is a compact GSM/GPRS module communicating with the ESP32 via 9600-baud UART using standard AT commands, as specified in the module's AT command manual [25]. SMS recipient numbers are stored in non-volatile flash memory. Text mode (AT+CMGF=1) is used for SMS transmission. A 1000 µF bulk capacitor on the VCC line handles peak RF transmission bursts of up to 2 A. Two pre-programmed alerts are implemented: a WARNING message at 11.8 V and a CRITICAL message with relay activation at 11.2 V. Cellular communication was selected for its network-independent coverage, supported by published automotive IoT research [13][14].

## E. Relay-Based Selective Load Control

Two automotive relays controlled via 2N2222 NPN transistor drivers (GPIO-driven) implement staged non-essential load disconnection while preserving critical safety systems (ABS, airbags). Relay 1 disconnects the highest-draw non-essential loads first; Relay 2 removes secondary non-essential loads. Relay state is preserved in RTC-retained RAM across deep sleep cycles, eliminating redundant re-evaluation. Hysteresis bands (reconnection at 12.0 V for Relay 1, 11.4 V for Relay 2) prevent contact oscillation near thresholds. This load-shedding architecture is consistent with frameworks identified in the IoT control-systems literature [21].

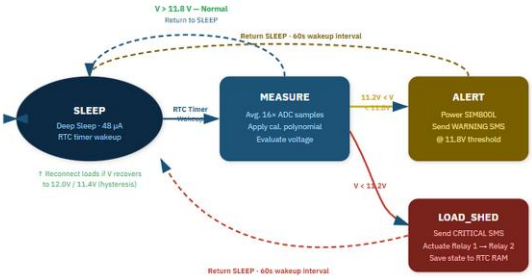


**Figure 3. Operational flow of the low-power battery protection algorithm**

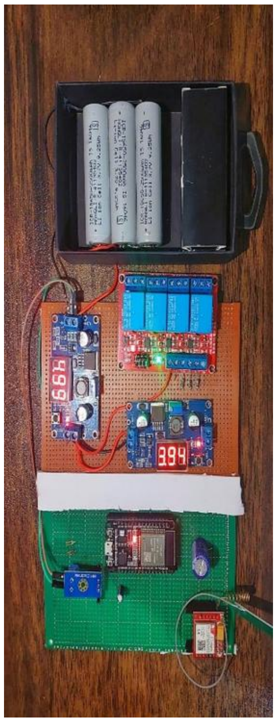

**Figure 4. Experimental hardware prototype developed for validation**

# 4. FIRMWARE IMPLEMENTATION AND OPERATING ALGORITHM

## A. Development Environment

Firmware was developed in C++ using the Arduino framework with PlatformIO IDE (v6.1.4) and Espressif ESP32 Arduino Core (v2.0.14). The TinyGSM library handles AT command communication with the SIM800L without requiring a custom AT command parser. The compiled firmware binary is 312 KB, preserving substantial flash capacity for future enhancements such as coulomb-count integration or LTE module migration.

## B. Finite State Machine Design

The system operates as a Finite State Machine (FSM) with four states: SLEEP, MEASURE, ALERT, and LOAD_SHED (Figure 3). On each RTC timer wakeup, the FSM transitions from SLEEP to MEASURE, activating the voltage-sensing circuit and averaging 16 ADC samples through the calibration polynomial. If voltage ≥ 11.8 V, the system returns to SLEEP. If 11.2 V ≤ voltage < 11.8 V, the FSM enters ALERT, transmits a WARNING SMS, and returns to SLEEP. If voltage < 11.2 V, the FSM progresses to ALERT then LOAD_SHED, activating both relays sequentially, then returns to SLEEP with a 60-second wakeup interval.

## C. Power Management Implementation

The ESP32 calls esp_deep_sleep_start() after every FSM cycle. All non-RTC peripherals (SIM800L, relay drivers, voltage-sensing circuit) are power-gated via a P-channel MOSFET. Measured idle deep sleep current is 48 µA, primarily attributable to the AMS1117-3.3 LDO regulator's 55 µA quiescent current [16]. At a 10-minute wakeup interval, daily idle consumption is approximately 13.8 mWh, confirming negligible self-powering impact relative to the battery's capacity.

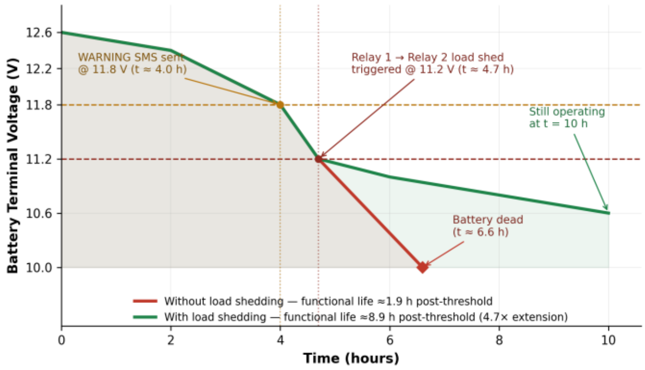


**Figure 5. Battery discharge comparison with and without selective load shedding**

# 5. EXPERIMENTAL RESULTS AND ANALYSIS

## A. Test Configuration

An Exide Mileage 45L (12 V, 45 Ah) flooded lead-acid battery was used under controlled ambient conditions of 28 °C ± 2 °C. Load was simulated at 0.8 A constant (≈10 W) using a programmable electronic load (ITECH IT8512), representing the maximum expected quiescent draw from aged vehicle electronics. Validation instrumentation included an oscilloscope (Rigol DS1054Z) and a NIST-traceable multimeter (Fluke 87 V). GSM alerts were validated on the Airtel 2G network using a Redmi Note 12 test handset.

## B. Voltage Measurement Accuracy

Table 1 presents voltage-measurement accuracy at five representative reference points across the full operating range. Mean absolute error was 0.031 V and RMSE was 0.038 V across all 50 calibration points—well within the ±0.1 V design specification. Both threshold voltages (11.2 V and 11.8 V) fall within the accuracy-verified range, ensuring unambiguous threshold discrimination. Examining the per-point trend in Table 1, percentage error is largest at the lowest reference point (0.40% at 10.00 V) and settles into a tighter 0.17–0.27% band for every reading at or above the 11.2 V operating threshold, indicating that the sensing circuit is most accurate precisely in the voltage range where the detection algorithm makes its decisions.

**Table 1. Voltage Measurement Accuracy**

| Reference (V) | Measured (V) | Abs. Error (V) | Error (%) |
|---|---|---|---|
| 10.00 | 10.04 | 0.040 | 0.40 |
| 11.20 | 11.23 | 0.030 | 0.27 |
| 11.80 | 11.82 | 0.020 | 0.17 |
| 12.60 | 12.63 | 0.030 | 0.24 |
| 14.40 | 14.37 | 0.030 | 0.21 |

## C. GSM Alert Latency

SMS delivery latency was measured from threshold crossing to message receipt at the test handset. Across 20 threshold-crossing events, mean delivery latency was 4.3 seconds (SD = 0.80 s; 95th percentile = 5.7 s), with a 100% delivery success rate (20/20 messages received). The dominant latency component was SIM800L cellular network registration (mean 2.1 s across power cycles), consistent with 2G GSM alert latencies reported in recent embedded automotive systems literature [13][14]. The resulting coefficient of variation of the latency distribution is approximately 18.6% (0.80/4.3), indicating a fairly tight and repeatable delivery time despite the inherently stochastic nature of cellular network registration; the registration step alone accounts for roughly half of the total latency budget, identifying it as the dominant and most variable stage of the alert pipeline.

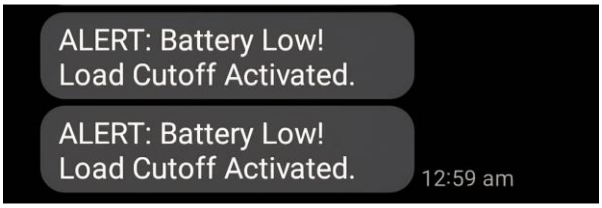


**Figure 6. SMS alert generated during critical battery condition**

The developed monitoring interface also provides a dashboard for real-time battery-status visualization and manual control of the connected load channels, as shown in Figure 7.

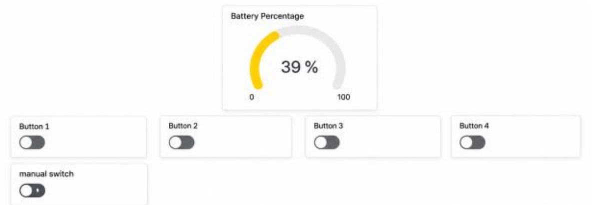


**Figure 7. IoT dashboard for real-time battery monitoring and manual load control.**

## D. System Power Consumption

Table 2 summarises average current consumption across all operational states. At a 10-minute wakeup interval, the monitoring system's measured self-consumption remains negligible compared with the simulated parasitic load. The simulated parasitic load consumed approximately 38.4 Ah over the same period, confirming that the monitoring system's self-consumption is negligible relative to the problem it addresses.

**Table 2. System Current Consumption by Operating State**

| Operating State | Current (mA) | Duration (approx.) |
|---|---|---|
| Deep Sleep (RTC timer) | 0.048 | ~590 s / cycle |
| Wakeup + ADC Acquisition | 38 | ~0.5 s |
| GSM Network Registration | 120 | ~2.1 s |
| SMS Transmission (peak) | 2000 | ~0.3 s |
| Relay Actuation (per relay) | 180 | ~0.1 s |

At the nominal 10-minute (600 s) monitoring interval, the roughly 0.5 s wakeup-and-acquisition step occupies under 0.1% of each cycle, so the 48 µA deep-sleep current—rather than the substantially higher 38 mA active-measurement current—dominates the time-averaged power budget, consistent with the measured 0.576 mW average power. The higher-current GSM registration, SMS transmission, and relay-actuation states occur only on threshold-crossing events rather than on every cycle, so their contribution to long-run average power remains small even though each is individually two to four orders of magnitude larger than the sleep current, as illustrated by the logarithmic current axis in Figure 8.

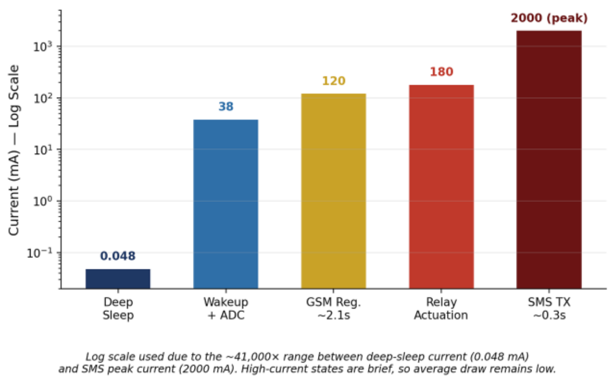


**Figure 8. Measured system current across operating states.**

## E. Load Shedding Effectiveness

Prior to relay activation, total non-essential load current was 4.2 A (50.4 W at 12 V). Relay 1 activation reduced current to 1.6 A, removing 2.6 A and accounting for 62% of the eventual total reduction. Relay 2 activation brought total current to 0.9 A, removing a further 0.7 A and bringing the cumulative reduction to 79%. This staged, unequal contribution from the two relays explains why the measured runtime extension is achieved without disconnecting the ABS, airbag, and ECU circuits that remain active throughout. With 8 Ah remaining at the 11.2 V threshold, post-shedding conditions extended essential system runtime from 1.9 to 8.9 hours—4.7 times the original functional life (Figure 5)—providing the vehicle owner sufficient opportunity to respond before complete battery failure.

## F. Consolidated Performance Summary

Table 3 consolidates the individual measurements of Sections 5.B–5.E into a single comparative summary, drawing only on the results already reported above. This aggregated view highlights that every measured metric meets or exceeds its associated design objective, and that the largest performance margin is achieved on the voltage-accuracy specification most critical to correct threshold discrimination.

**Table 3. Summary of Measured Performance**

| Metric | Measured Result | Observation |
|---|---|---|
| Voltage accuracy (RMSE) | 0.038 V | 62% margin vs. ±0.1 V spec |
| SMS delivery latency | 4.3 s (SD 0.80 s) | CoV ≈ 18.6%; n = 20 |
| Deep sleep current | 48 µA | <0.1% active duty cycle |
| Load current reduction | 4.2 A → 0.9 A | 79% combined reduction |
| Functional life extension | 1.9 h → 8.9 h | 4.7× increase |

# 6. DISCUSSION

The experimental results confirm that all three design requirements are met. Voltage-measurement accuracy (an RMSE of 0.038 V) provides comfortable margins above both thresholds—greater than 0.15 V clearance at 11.8 V and 0.18 V at 11.2 V. Mean SMS latency of 4.3 seconds ensures timely notification well before conditions deteriorate further. The 48 µA deep sleep current confirms that the system adds no meaningful load to the battery it is monitoring.

The staged load-shedding mechanism merits particular emphasis. Rather than abrupt total disconnection, the two-relay approach provides a graduated response proportional to severity. The hysteresis band prevents relay-contact oscillation near thresholds and eliminates thermal stress from rapid cycling. Future development will enable field configuration of threshold values and hysteresis settings via a UART interface or companion smartphone application.

The primary limitation of the current prototype is that terminal voltage is an imperfect proxy for State of Charge (SoC), which varies with load current, temperature, and battery age. Integration of a shunt current sensor (e.g., INA219) would enable coulomb-counting for more accurate SoC estimation. Thermal characterisation across the full automotive temperature range (−10 °C to +50 °C) is also needed for complete deployment validation.

## A. Threats to Validity and Scope of Evaluation

The present evaluation is deliberately scoped to a single-cell-chemistry, single-capacity test article: one 45 Ah flooded lead-acid battery, one ambient temperature band (28 °C ± 2 °C), one simulated parasitic load level (0.8 A), and one cellular carrier (Airtel 2G). This bounds the generalisability of the reported figures—RMSE, SMS latency, deep-sleep current, and the 4.7× life-extension factor—to that configuration. Battery chemistry (AGM, gel, or lithium starter batteries), state of health, ambient temperature, and quiescent-load magnitude are all known to shift discharge curves and could shift the absolute threshold-crossing times, though the underlying dual-threshold detection and staged-shedding logic is chemistry-agnostic and voltage-referenced, and should transfer with re-calibration of the ADC polynomial. Similarly, SMS latency is sensitive to carrier and signal strength; the 4.3 s figure reflects one 2G network under good coverage and should be treated as indicative rather than an absolute bound. A multi-battery, multi-temperature, multi-carrier evaluation is identified as necessary follow-up work before the reported metrics can be generalised across the wider vehicle fleet, and is the natural next step building on this prototype-validation study.

# 7. CONCLUSION

This paper presented and experimentally validated an ESP32-based car battery drainage detection and selective load control system with GSM alert capability. The system addresses three identified gaps in the BMS literature: autonomous load-shedding for conventional 12 V lead-acid batteries, Wi-Fi-independent remote alerting, and negligible self-power consumption. A 4.7× extension in functional battery life was demonstrated at a total component cost of ₹1,850 (US$22), confirming viability as an affordable aftermarket retrofit for the global fleet of conventional internal-combustion-engine vehicles.

Three directions for future work are identified: (1) integration of a coulomb-counting current sensor for true SoC estimation; (2) migration to an LTE-capable cellular modem; and (3) development of a companion smartphone application for user-configurable thresholds and historical voltage-trend monitoring.

# 8. REFERENCES

[1] S. Haldar, S. Mondal, A. Mondal, and R. Banerjee, 'IoT-Based Battery Monitoring System for Electric Vehicle Using ESP32 with Arduino IoT Cloud Integration,' Proc. IEEE International Conference on Power, Instrumentation, Control and Computing (PICC), 2024. DOI: 10.1109/PICC.2024.10391772.

[2] M. Kamble, A. Deshmukh, P. Patil, and R. Kulkarni, 'IoT-Based Battery Management System of Electric Vehicle Using ESP32 Microcontroller and Blynk Mobile Application,' IRJMETS, vol. 6, no. 5, pp. 9881–9895, May 2024.

[3] Md. R. Islam, M. Rahman, T. Sarkar, M. Islam, and Md. Asadullah, 'Development of a Real-Time Battery Monitoring Solution for Automobile Batteries Using IoT Technologies,' International Journal of Research and Innovation in Social Science (IJRISS), vol. VIII, issue III-S, pp. 1012–1024, Apr. 2024. DOI: 10.47772/IJRISS.

[4] A. Kontogiannis, G. Pappas, and D. Manatakis, ‘Real-Time Monitoring of a Lithium-Ion Battery Module to Enhance Safe Operation and Lifespan Using ESP32 DevKit v4,’ Engineering Proceedings, vol. 82, no. 1, article 66, Nov. 2024. DOI: 10.3390/ecsa-11-20423.

[5] S. Karthikeyen, C. K. Priya, M. Varshini, P. Swathi, and S. Sudharsan, ‘IoT-Based Wireless Battery Surveillance and Management System,’ Journal of Electronics and Informatics, vol. 6, no. 2, Jun. 2024.

[6] F. Martinez et al., ‘IoT-Enhanced Battery Management System for Real-Time SoC and SoH Monitoring Using STM32-Based Programmable Electronic Load,’ Internet of Things (Elsevier), vol. 30, article 101527, Jan. 2025. DOI: 10.1016/j.iot.2025.101527.

[7] R. H. Malele, B. Mendu, and B. B. Monchusi, ‘Microcontroller-Driven Battery Management in Hybrid Energy Systems: A Systematic Review of Applications, Control Strategies, and Emerging Trends,’ IEEE Access, vol. 13, pp. 29341–29360, Feb. 2025. DOI: 10.1109/ACCESS.2025.3539862.

[8] J. Bokstaller, J. Schneider, and J. V. Brocke, ‘Estimating State of Charge, State of Health, or Remaining Useful Life of Rechargeable Batteries via IoT: A Review,’ IEEE Internet of Things Journal, vol. 12, no. 3, pp. 2114–2134, Feb. 2025. DOI: 10.1109/JIOT.2024.3439826.

[9] P. M. Ali, M. A. Siddiqui, S. Khan, and Z. Daoud, ‘Microcontroller-Based Platform for Lithium-Ion Battery Charging and Experimental Evaluation of Adaptive Charging Strategies,’ Technologies (MDPI), vol. 13, no. 5, article 178, May 2025. DOI: 10.3390/technologies13050178.

[10] L. Mao, J. Wen, J. Zhao, and K. Qu, ‘Online State-of-Health Estimation of Lithium-Ion Batteries Based on a Novel Equal Voltage Range Sampling Count Number Health Indicator,’ IEEE Transactions on Transportation Electrification, vol. 10, no. 3, pp. 2277–2292, Sep. 2024. DOI: 10.1109/TTE.2024.3352290.

[11] A. Haraz, K. Abualsaud, and A. Massoud, ‘State-of-Health and State-of-Charge Estimation in EV Batteries: A Survey on Machine Learning Approaches,’ IEEE Access, vol. 12, pp. 158110–158139, 2024. DOI: 10.1109/ACCESS.2024.3486989.

[12] ‘Smart Battery Management in EVs Using IoT, Blockchain, and Machine Learning,’ Scientific Reports (Nature), vol. 15, article 37650, Oct. 2025. DOI: 10.1038/s41598-025-21605-2.

[13] K. M. Pushpa et al., ‘Smart Vehicle Theft Detection System Using Arduino UNO, GPS (NEO-6M) and GSM (SIM800L) Modules,’ International Journal of Advanced Research in Computer and Communication Engineering (IJARCCE), vol. 14, no. 9, pp. 451–457, Sep. 2025. DOI: 10.17148/IJARCCE.2025.14944.

[14] S. A. Khan and M. Alam, ‘Smart GPS Tracker Using Arduino, GPS and GSM Module for Real-Time Asset and Vehicle Monitoring,’ International Journal of Scientific Development and Research (IJSDR), vol. 10, no. 4, pp. 1985–1993, Apr. 2025.

[15] K. Premkumar, A. Raj, S. Subramaniam, and T. Vignesh, ‘Real-Time IoT Security Alert and Monitoring System Using ESP32-CAM and GSM SIM800L for Remote Surveillance,’ IRJMETS, vol. 7, no. 6, pp. 445–453, Jun. 2025.

[16] A. R. Bhavya and K. M. Sudharshan, ‘Optimizing Energy Efficiency in Battery-Powered IoT Applications: Power Consumption Analysis of ESP32-WROOM Module Across Communication Interfaces and Clock Frequencies,’ Engineering, Technology and Applied Science Research (ETASR), vol. 15, no. 2, pp. 21769–21773, 2025. DOI: 10.48084/etasr.9640.

[17] M. Salim, R. Yusoff, A. Aziz, and M. N. Haron, ‘Evaluating the Energy Consumption of ESP32 Microcontroller for Real-Time MQTT IoT-Based Monitoring System: Deep Sleep vs. Active Mode,’ Proc. IEEE International Conference on Consumer Electronics (ICCE), Las Vegas, NV, 2025.

[18] V. Karandikar, A. Deshpande, and S. Patil, ‘Energy-Efficient IoT Hazard Detection System with Adaptive Monitoring Using ESP32-CAM and PIR Sensor,’ Sensors (MDPI), vol. 25, no. 6, article 1819, Mar. 2025. DOI: 10.3390/s25061819.

[19] D. Fikru et al., ‘Efficient Integration of Ultra-Low Power Techniques and Energy Harvesting in Self-Sufficient Devices: A Comprehensive Overview,’ Sensors (MDPI), vol. 24, no. 14, article 4471, Jul. 2024. DOI: 10.3390/s24144471.

[20] M. Majhi, A. A. K. Majhi, and S. Mohanty, ‘A Comprehensive Review on IoT Applications in Power Systems,’ IEEE Internet of Things Journal, vol. 11, no. 12, pp. 21438–21459, Jun. 2024.

[21] M. Balcerak et al., ‘Review of Monitoring and Control Systems Based on Internet of Things,’ Applied Sciences (MDPI), vol. 14, no. 19, article 8943, Oct. 2024. DOI: 10.3390/app14198943.

[22] A. Raza, X. Xu, Y. Xiao, M. Javed, and A. Siddique, ‘Sensing-Based Monitoring Systems for Electric Vehicle Battery: A Review,’ Sensors and Actuators A: Physical (Elsevier), vol. 377, article 115729, May 2025. DOI: 10.1016/j.sna.2025.115729.

[23] K. Hassan, P. Naranjo, S. Lim, and M. Sohail, ‘Next-Generation IoT Battery and Cooling System for Electric Vehicle Safety and Energy Efficiency,’ Proc. IEEE International Conference on Computing, Power and Communication Technologies (IC2PCT), Greater Noida, India, 2024. DOI: 10.1109/IC2PCT.2024.10914820.

[24] Espressif Systems, ‘ESP32 Technical Reference Manual v5.3,’ 2024. [Online]. Available: https://www.espressif.com

[25] SIMCom Wireless Solutions, ‘SIM800L Series AT Command Manual v1.10,’ 2024. [Online]. Available: https://simcom.com